

Mechanical Behavior and Microstructural Correlations in a TRIP Assisted Bainitic Steel

JN Mohapatra*, Satish Kumar Dabirur and G Balachandran

R & D, JSW Steel Ltd, Toranagallu-583275, India

ISSN: 2576-8840



*Corresponding author: JN Mohapatra, R & D, JSW Steel Ltd, Toranagallu-583275, India

Submission: 📅 July 28, 2022

Published: 📅 August 05, 2022

Volume 17 - Issue 4

How to cite this article: JN Mohapatra*, Satish Kumar Dabirur, G Balachandran. Mechanical Behavior and Microstructural Correlations in a TRIP Assisted Bainitic Steel. Res Dev Material Sci. 17(4). RDMS. 000916. 2022.
DOI: [10.31031/RDMS.2022.17.000916](https://doi.org/10.31031/RDMS.2022.17.000916)

Copyright@ JN Mohapatra. This article is distributed under the terms of the Creative Commons Attribution 4.0 International License, which permits unrestricted use and redistribution provided that the original author and source are credited.

Abstract

A lean alloyed steel of 0.17%C, 1.73% Mn, 1.35% Si along with 0.02% Nb, 0.04%Ti as microalloying additives was pre hardened and subjected to TRIP assisted bainitic steel heat treatment. The pre hardening treatment from 950 °C promotes the formation of carbide free bainite in lath form in addition to blocky form which enhance the steel properties. The steel was austenitized at 790 and 830 °C followed by austempering at 450 °C. The steel developed a microstructure consisting of inter critical ferrite, bainitic ferrite, Martensite/ austenite constituents along with significant quantities (12 to 17%) of retained austenite. The microstructural phase evolution was compared with the theoretically assessed results. The mechanical properties of the steel showed that the steel developed a tensile strength in the range 766 to 968MPa with 20 to 29% elongation and yield ratio varying between 0.57 to 0.72. The tensile toughness of the steel was 17.3 to 23.7GPa %. The work hardening behavior of the steel was examined using the Hollomon equation and the modified Crussard Jaoul equations.

Keywords: Pre hardening heat treatment; TRIP assisted bainitic steel; Microstructure; Mechanical properties; Work hardening; Crussard jaoul model

Introduction

TRIP steels are unique materials that has excellent combination of strength and ductility [1-7]. There is a search for development of third generation mechanical properties in such steel where the product of strength and ductility exceed 20GPa.%. The steels for automotive applications are usually low carbon - manganese steel additionally alloyed with Si content close to 1.5%. These steels are alloyed with Mn, Ni, Cr and Mo to improve the hardenability, and retained austenite stability. The steels are further alloyed with grain refining elements; Ti, Nb or V to achieve fine grain sizes that enhances the strength and toughness and a higher homogeneity in the microstructure. The properties in the steels are governed by the carbon content in the alloy, and the alloying elements. Properties range from TRIP 590 to as large as TRIP 1180 in commercialized steels.

The TRIP steel processing involves holding the steel in the inter critical heat treatment regime, where there is a partition of carbon between ferrite and austenite that leads to a carbon rich austenite that has an M_s temperature lower than that of the steel M_s temperature. This inter critical holding is followed by austempering in the bainitic region, to transform the carbon rich austenite to bainitic ferrite, retained austenite/ martensite phases. The steel gives excellent properties in this condition.

The objective of the present study is to examine the evolution of microstructure and mechanical properties in a pre-hardened TRIP steel austempered at various temperatures in a lean steel composition. The work hardening behavior of the steel were examined to understand the hardening mechanism.

Experimental

A hot rolled steel of 3mm thickness produced at JSW Steel Ltd, Vijaynagar Works was used for the study. The chemical composition of the steel was examined using SPECTRO make optical emission spectrometer as shown in Table 1. Cut steel strip 30mm width and 300mm length were subjected to laboratory scale heat treatment, as per cycle shown in Figure 1. It involves heating the cut strip to above A_{c3} temperature (950 °C), holding for 20min and water quenched. Such quenched steel was subjected to inter critical austenitization at 790 °C and 830 °C, both hold for 20min, followed by quenching to salt bath maintained at temperatures of 300, 350, 400, 425,

and 450 °C hold for 15min followed by water quenching. Tensile specimens were prepared in JIS standard and tested with the use of video extensometer in a Zwick make 250kN tensile testing machine with 50mm GL and at a strain rate of 0.008/s. Microstructure and SEM micrographs, were carried out in an opto-digital microscope of Olympus make and Hitachi Make SEM respectively. The gray levels in the Lepera etched samples had distinct colours that distinguished the phases in optical metallography. PANlytical make XRD was used for determination of retained austenite content in the heat-treated samples.

Table 1: Chemical composition (wt. %) of the steel and its critical temperatures.

C	Mn	Si	S	P	N	Al	Ti	Nb
0.17	1.72	1.35	0.003	0.016	0.005	0.06	0.04	0.02
$A_{c3}=875\text{ }^{\circ}\text{C}$, $A_{c1}=731\text{ }^{\circ}\text{C}$, $B_s=557\text{ }^{\circ}\text{C}$ & $M_s=417\text{ }^{\circ}\text{C}$								

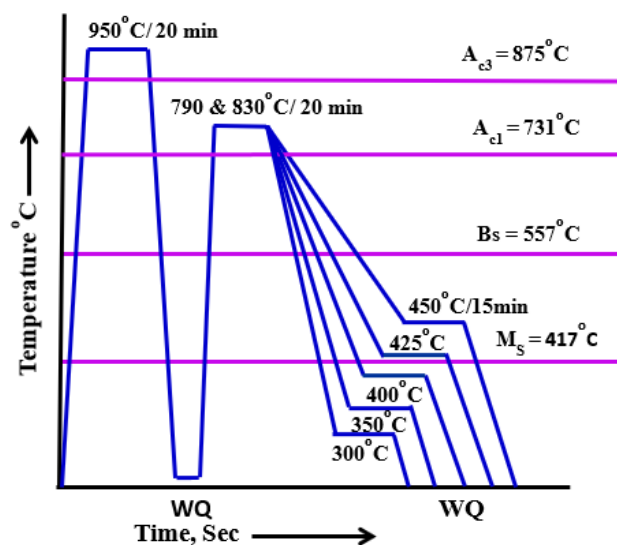


Figure 1: Heat treatment cycle carried out on the sample.

Results and Discussion

The steel, used in the present study is a lean alloyed composition with microalloying additives Ti and Nb that refine the grain size. The steel has good formability and weldability associated with low carbon content. The presence of 1.72% Mn ensures that A_{c1} temperature is lowered, and the austenite fraction increases at inter critical annealing treatment. Mn addition enhances hardenability and stability of the austenite that forms in the final steel after austempering. Nb, Ti and Al in the steels promote carbides and nitrides that refine the steel grain sizes.

In the present study, the heat treatment cycle, as in Figure 1, has been carried with a prior quenching heat treatment. Such a pre quenching treatment is reported to nucleate austenite in the idiomorphic fashion along the prior austenite grain boundaries

along with accicular austenite formation between the martensite plates [7,8]. The prior quenched steel is reported to form more stable acicular austenite and it is reported to have high carbon concentration and hence stabilizes the retained austenite better [7]. The mechanical properties obtained are reported to be superior to the conventional TRIP steel without prehardening [7]. Hence, the heat treatment cycle includes prior quenching.

Inter critical annealing at 790 and 830 °C, post pre quenching, promote inter critical ferrite, the proportion of which increases with lower temperature, along with equilibrium austenite. The pseudo-binary phase diagram for the steel as assessed from Thermocalc software (2020b) is shown in Figure 2. Using the Lever rule in Figure 2, the ferrite phase fraction formed at the inter critical temperatures of 790 and 830 °C was assessed to be 43% and 71%,

respectively. At the inter critical austenitization, the carbon rejected by the low carbon ferrite enriches the austenite. Assuming 0.03% C as the solubility of carbon in the ferrite, the carbon enrichment in austenite was found to be 0.36% C at 790 °C and 0.23% at 830 °C by mass balance. The carbon enrichment in austenite, decreases the M_s temperature of the residual austenite, which was found to be 324 °C for the 790 °C austenite fraction and 379 °C for the 830 °C austenite fraction. The inter critically austenitized steel, was subjected to austempering in a salt bath between 300 and 450 °C held for 15min holding time (Figure 1). During the austempering heat treatment, the carbon rich austenite fraction decomposes to ferritic bainite phase up to a certain limit decided by the T_0' temperature. The bainitic reaction stops at a temperature T_0' , at which the chemical potential of ferrite and austenite become equal, and the strains associated with transformation were included. Post the austempering treatment, the steels are quenched in water, which may either transform to martensite or may remain as retained austenite based on the austenite stability achieved by carbon enrichment.

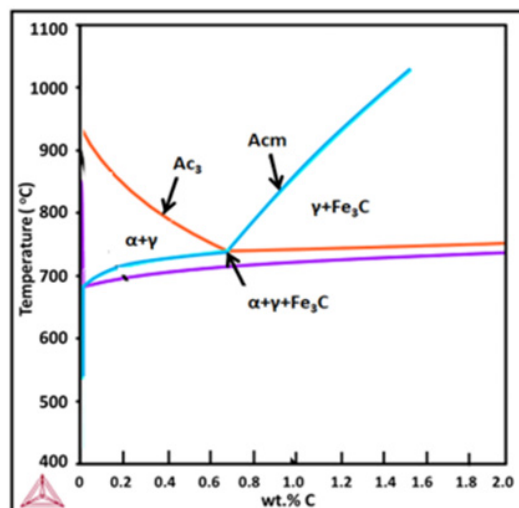


Figure 2: Phase diagram of the steel as a function of carbon content.

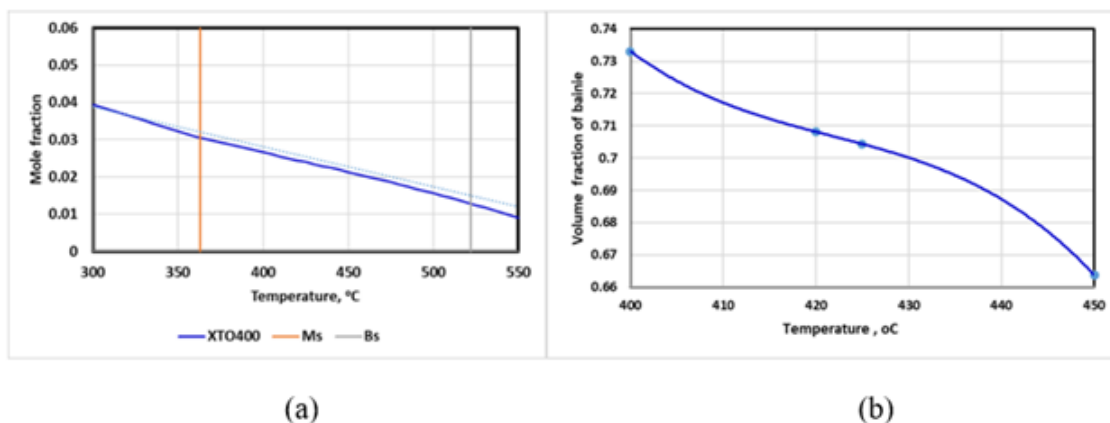


Figure 3: (a) Theoretical T_0' temperature for the steel evolved using Cambridge University software MUCG 83 [9]; (b) Calculated maximum volume % bainite as a function of austempering temperature at inter critical austenitization at 830 °C.

The limits to the bainitic transformation as determined by software MUCG83 [9] was found by evaluating the composition and T_0' temperature as in Figure 3(a). Using that, it was possible to find the volume percentage of bainite that would form at the isothermal hold temperatures of 450 °C from the mole fractions of the steel, carbon in ferrite (0.03% assumed), and mole fraction at the T_0' temperature. At the chosen austempering temperature, the amount of bainite that may form is found and the residual austenite that has not transformed to bainitic ferrite forms, blocky ferrite in the matrix. It is seen for the present composition, the lean alloyed steel has maximum bainite formation less than 78% in the entire range of austempering. It is for this reason; the steels are usually enriched with alloying elements such as Cr and Mo that enhances the volume of bainite formation during austempering.

Microstructure and phase analysis

The optical microstructure of the steel at various heat-treated condition is shown in Figure 4(a)-(f) and the corresponding SEM

microstructure in Figure 5(a)-(f). The optical microstructures show fine bainite with blocky inter critical ferrite. Larger fraction of blocky ferrite is seen at 790 °C, austenitization than the austenitization 830 °C, as expected. However, the morphology of the inter critical ferrite at 790 °C was blocky during the austempering at 300 and 400 C, while it is lath like when austempering at 450 °C. This may be related to higher bainite fraction that tend to form at close to bainite start temperature where the bainite fraction is the largest (Figure 3(b)). As the phase fraction estimation was inaccurate with optical micrography, SEM micrographs were used to examine the phases. There were at least two micrographs in each condition examined with an artificial grid and at least three locations in each micrograph the quantification was carried out. The phases were manually counted for each phase. The phases quantified include the gray ferrite phase, martensite/austenite constituent, bainite and retained austenite. The retained austenite was considered as the bright white films. This may be inaccurate as carbides are also bright white. In the present case all bright filmy

phase was considered as austenite. The phase fractions determined is shown in Table 2.

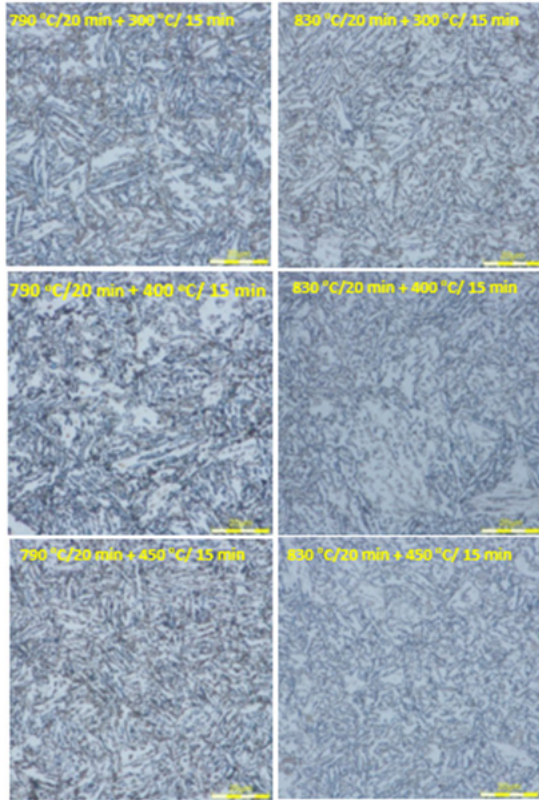


Figure 4: Optical microstructure of the steel at different heat-treated conditions.

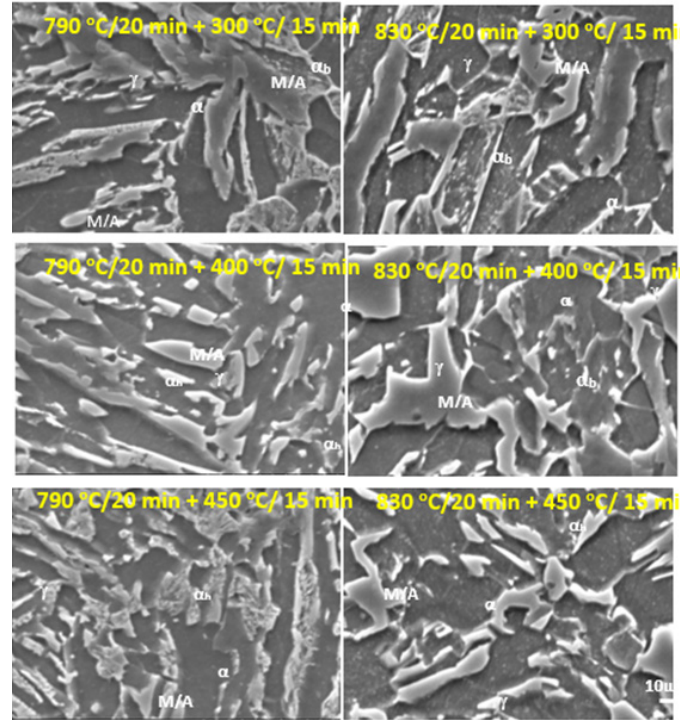


Figure 5: Typical SEM microstructure of the steel at the different heat-treated conditions (phases marked: α -ferrite; α' -martensite; α_b -bainitic ferrite; γ -retained austenite)

Table 2: Heat treatment condition and volume fraction of phase using SEM micrographs.

Inter-critical temperature in °C held for 20min	Aus-temper temp °C, for 15min	Theoretical Inter-critical % Ferrite	Measured ferrite	Theoretical % Aus-tenite	Theoretical % C in aus-tenite	Calcu-lated Ms	Max% Volume bainite MUGG 83	Theoretical % bainite	Measured bainite %	Residual austenite after austempering %	SEM Measured Residual austenite after cooling to RT	Measured XRD Retained austenite	SEM Measured martensite after cooling to RT
830	300	43	44.85	57	0.28	363	100	29	33.33	37.87	10.28		17.69
830	350	43	46.09	57	0.28	363	100	29	37.86	15.23	11.11	12.16	4.52
830	400	43	52.26	57	0.28	363	100	29	14.81	36.22	14.40	10.32	23
830	420	43	58.43	57	0.28	363	0	0	19.33	34.34	5.76	13.21	10.69
830	450	43	51.02	57	0.28	363	0	0	16.46	20.17	18.10		17.33
790	300	71	28.8	29	0.54	249	0	0	25.51	29.64	12.76		11.93
790	350	71	46.91	29	0.54	249	0	0	30.86	23.05	12.75	12.16	13.16
790	400	71	48.97	29	0.54	249	73.3	41.78	17.28	30.46	11.93		22.63
790	425	71	46.33	29	0.54	249	70.8	40.36	24.69	16.88	8.64	18.31	9.05
790	450	71	63.37	29	0.54	249	66.37	37.83	45.26	3.72	2.46	< 4.0	3.7

The optical microstructure of the steel at 790 and 830 °C, austenitized at different austempering temperature shows inter critical ferrite, which is blocky. Since lath martensite is the starting microstructure before TRIP heat treatment, the low temperature

austenitization shows fine globular bainite within the blocky inter critical ferrite. These fine features enhance the strength and ductility of the steel. Other than blocky ferrite, brownish bainite phase in lath shape is shown. The optical microstructure could not

give retained austenite, as it occurs as thin films around martensite lath boundaries as observed in SEM micrographs (Figure 5). The SEM micrographs reveal the distinct phases at each heat treatment conditions are plotted in Figure 6. Ferrite, bainitic ferrite and M/A constituents are clearly revealed. The martensite phase is

associated with a thin and bright white retained austenite. The bainite zones are finer at 790 °C compared to 830 °C. Thin bright room temperature stabilized austenite is found evenly distributed in the matrix.

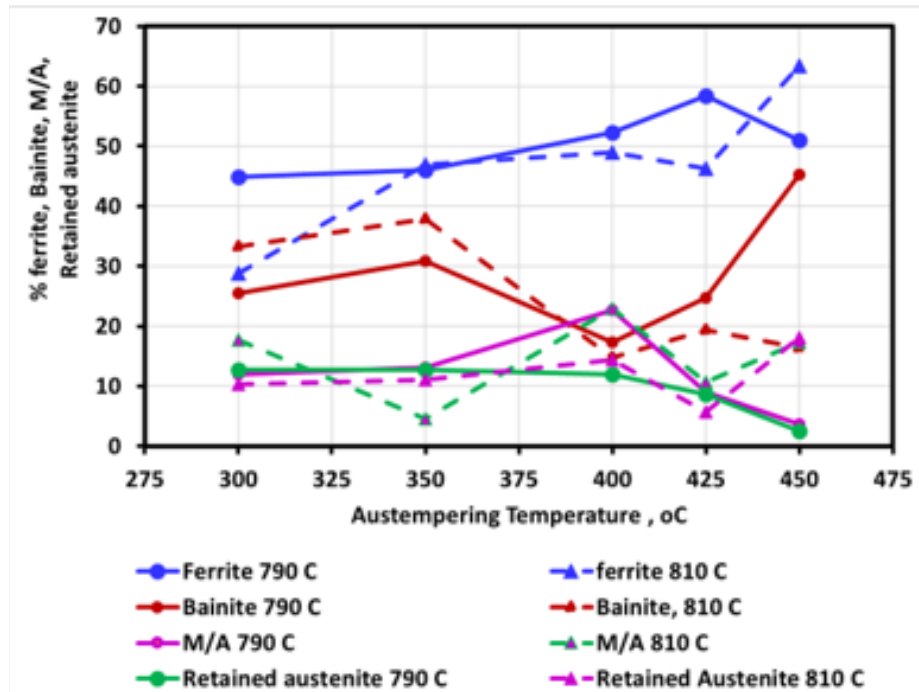


Figure 6: Volume fraction of the phases as a function of austempering temperature measured by SEM phase analysis.

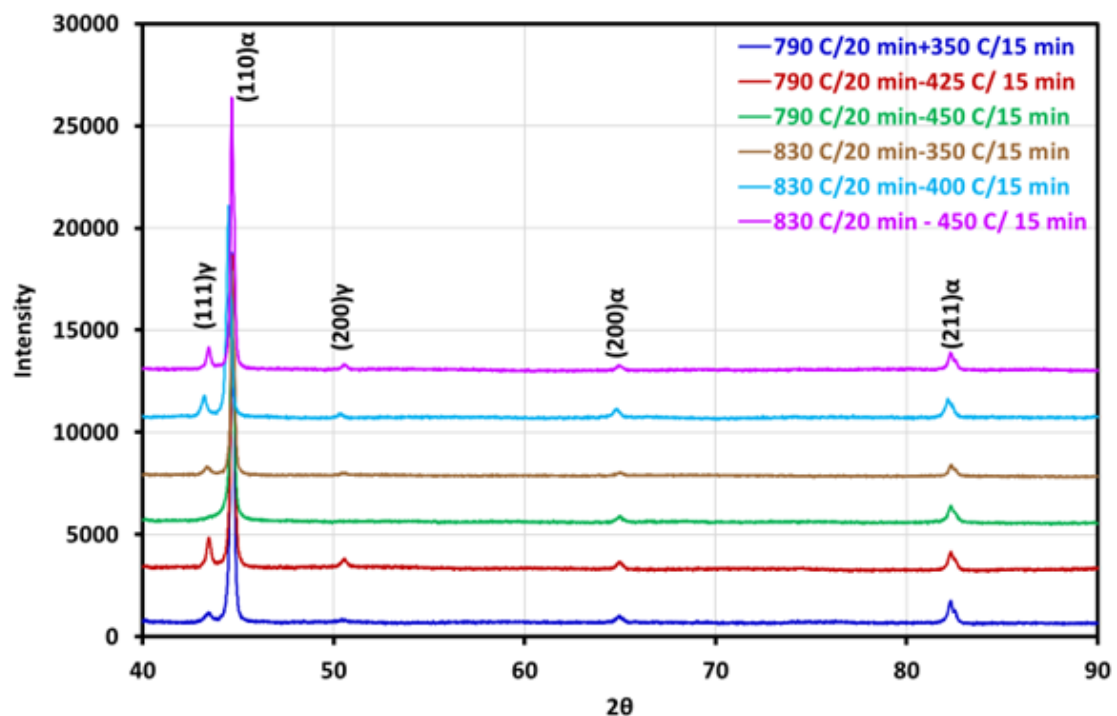


Figure 7: XRD pattern of the samples studied showing significant austenite peaks (Note intensity has been progressively magnified by 5000 units among each XRD pattern).

The evolution of the microstructure was examined by calculating (Table 2) the inter critical % ferrite for phase diagram using Lever rule in Figure 2. The inter critical ferrite formed as per equilibrium calculation for 790 °C is higher compared to 830 °C. The corresponding austenite fraction is lower, and it is more enriched with carbon than in 830 °C austenitized samples. Depending on carbon enrichment the M_s and B_s temperature decreases. During austempering, the residual inter critical austenite undergoes bainitic transformation at the chosen austempering temperature. As the extent of bainitic reaction is decided by T_0' temperature, the bainite reaction proceeds till the composition reached that in the T_0' temperature. This was determined for both the range of inter critical temperature and at every austempering temperatures using the Cambridge software MUCG83 for the carbon enriched austenite. In the case of 790 °C austenitized samples the significant carbon enrichment results in 100% bainite formation while for 830 °C the bainite volume fraction is limited. There is significant retained austenite for 830 °C post austempering treatment (Figure 7). During subsequent water quenching the unstable austenite if any undergoes secondary bainite or martensite transformation. The

theoretically determined phase fraction and the measured values showed significant differences. The measured ferrite fraction was lower in 790 °C. The bainite content is higher at 790 °C. The pre hardening treatment seems to be affecting the microstructural features that probably alters the theoretically calculated data.

Mechanical properties post heat treatment

The stress-strain diagram of the steel at various heat treatment conditions is shown in Figure 8. The heat treatment conditions and mechanical properties at various conditions is shown in Table 3. It is seen that the tensile strength is moderately higher in the steel austenitized at 790 °C compared to that at 830 °C, especially at higher austenitizing temperature of 400 to 450 °C. This may be attributed to the higher bainite fraction seen in the steel austenitized at 790 °C (Figure 9). The yield strength and elongation values at 790 and 830 °C austenitization followed by austempering are very close. Although marginal, the tensile strength values are lowest at 350 °C and yield strength peaks at about 375 °C (Figure 9). The elongation value peaks at 400 °C. The yield ratio is higher for 830 °C austenitization than that for 790 °C (Table 3). The yield ratio peaks at 350 °C with a value of 0.71 (Figure 10).

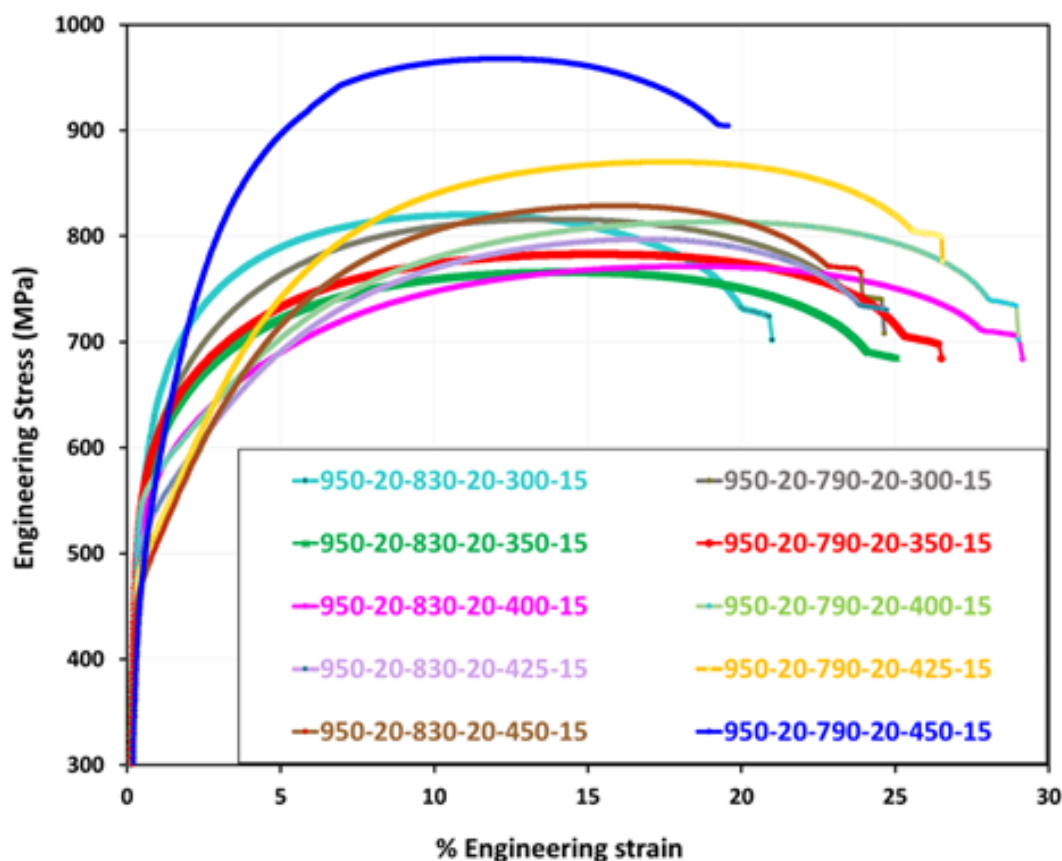


Figure 8: Stress-strain diagram of the steel at various heat treatment conditions.

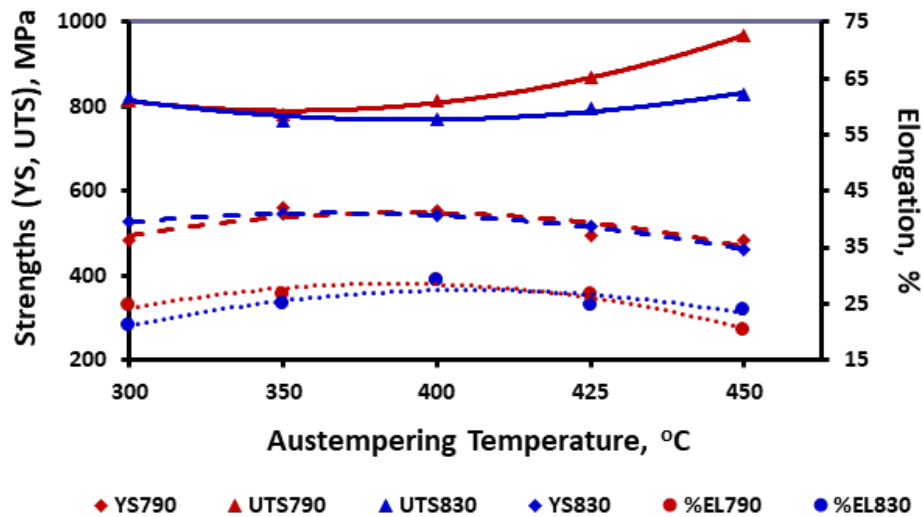


Figure 9: The mechanical properties of the steel at the different austempering temperatures.

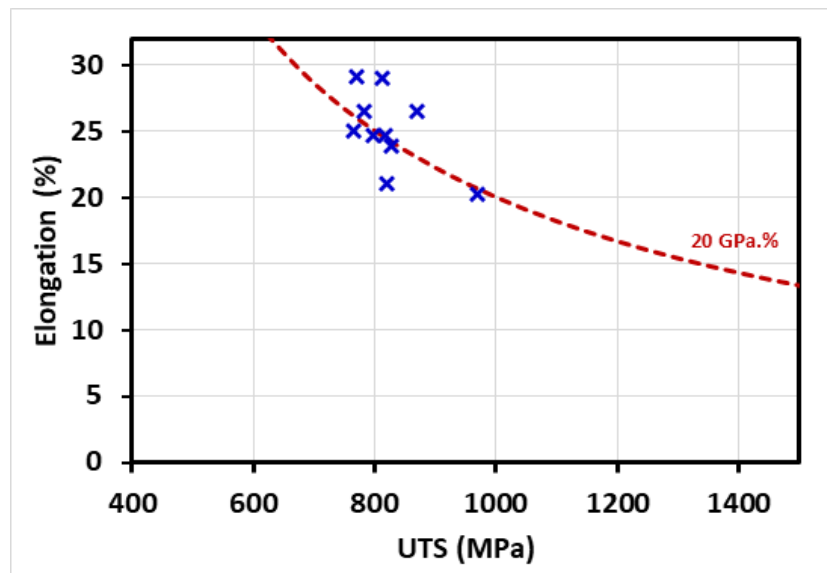


Figure 10: The strength and ductility relation of the present study show that the n AHSS property range.

Table 3: Heat treatment condition and mechanical properties of the steel.

Heat Treatment Condition						Mechanical Properties				
Austenization above A _{cs} , WQ		Inter critical austenitization		Austempering, WQ		YS (MPa)	TS (MPa)	El. (%)	Yield Ratio	UTS*%E (GPa.%)
Temp °C	Time Min	Temp °C	Time Min	Temp °C	Time Min					
950	20	790	20	300	15	482	816	24.7	0.59	20.1
950	20	790	20	350	15	561	783	26.5	0.72	20.8
950	20	790	20	400	15	554	813	29.0	0.68	23.6
950	20	790	20	425	15	494	870	26.6	0.57	23.1
950	20	790	20	450	15	483	968	20.3	0.50	19.6
950	20	830	20	300	15	526	820	21.0	0.64	17.2
950	20	830	20	350	15	547	766	25.0	0.71	19.2

950	20	830	20	400	15	541	771	29.2	0.70	22.5
950	20	830	20	425	15	516	797	24.7	0.65	19.7
950	20	830	20	450	15	462	828	23.9	0.56	19.8

The properties of the steel is due to the strengthening associated with the multiphase microstructure that consists of inter critical polygonal ferrite, ferritic bainite phase, M/A constituents and the retained austenite content. The tensile strength values at 790 °C austenitization lie in a range 783 to 968MPa, while the corresponding ductility values lie between 20 and 29% elongation. Similarly, the strength values at 810 °C austenitization shows a tensile strength in the range between 771 to 828 with corresponding ductility between 21 and 29% elongation.

The strength is directly related to the proportion and distribution of the phases. However, there is scatter in the phase constitution and its direct correlation with strength could not be arrived. But the presence of significant amount of retained austenite implies that the steel could respond to the TRIP effect. The specific property of 968 MPa tensile strength with 20% elongation gives a light weight formable steel, which will be desired by automotive industry. The low temperature austenitization in the inter critical zone recrystallized the grains much finer than without quenching heat treatment. Within ferrite zones, fine globular bainite are observed which has improved ductility considerably.

The work hardening characteristics of the steels were assessed using the Hollomon equation

$$\sigma = K\varepsilon^n \quad (1)$$

where σ is the true stress, ε is true strain and n the work hardening exponent and K the strength coefficient. The slopes in the logarithmic equation gives the n value.

$$\ln(\sigma) = \ln(K) + n \ln(\varepsilon) \quad (2)$$

The plots so made in Figure 11(a) shows three distinct slopes. The initial hardening takes place by the dislocation movement in the ferrite phase till a critical strain where the dislocations multiply and harden the steel. Beyond the critical strain the dislocation moves in the ferritic bainitic phase along with the ferrite phase leading to a steep rise in the hardening. This takes place till the second critical strain beyond which the harder phases such as retained austenite and the M/A constituent start deforming leading to further hardening. The strain hardening coefficient variation as a function of austempering temperature is shown in Figure 11(b).

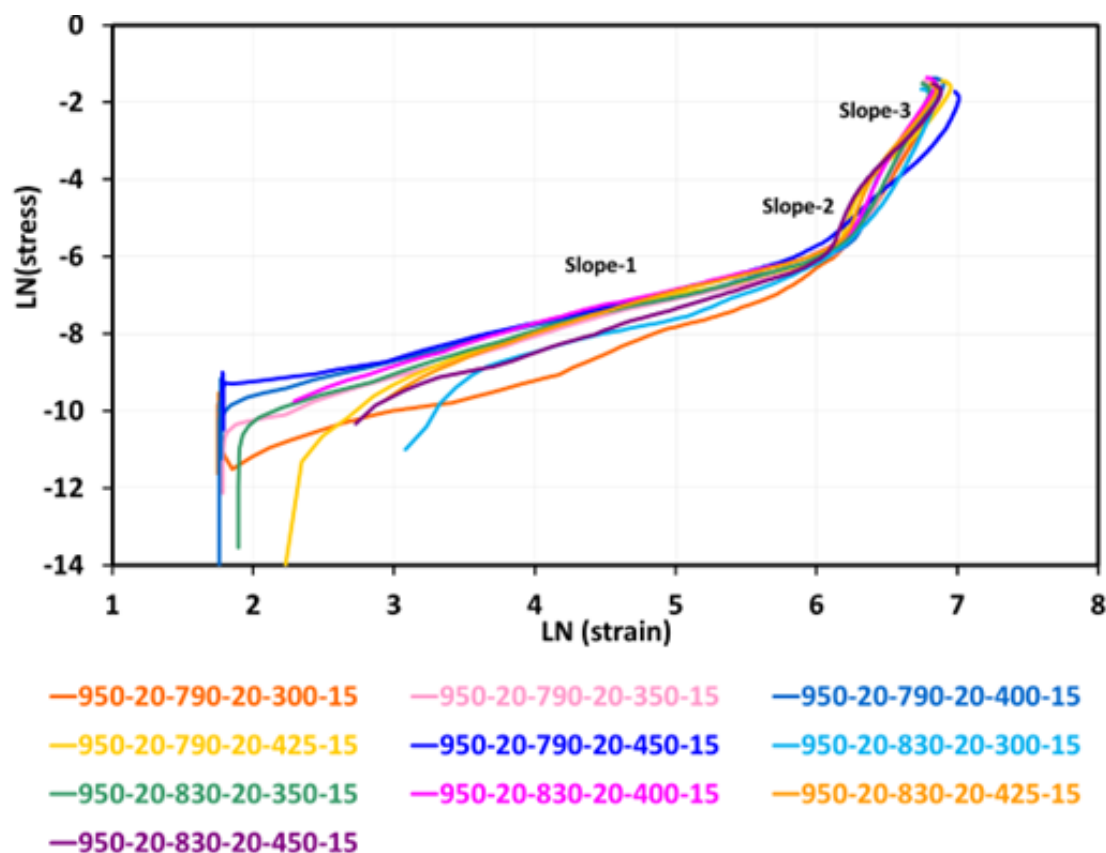


Figure 11(a): The work hardening of the steel at the various processing conditions as per Hollomon equation ($\sigma = K\varepsilon^n$).

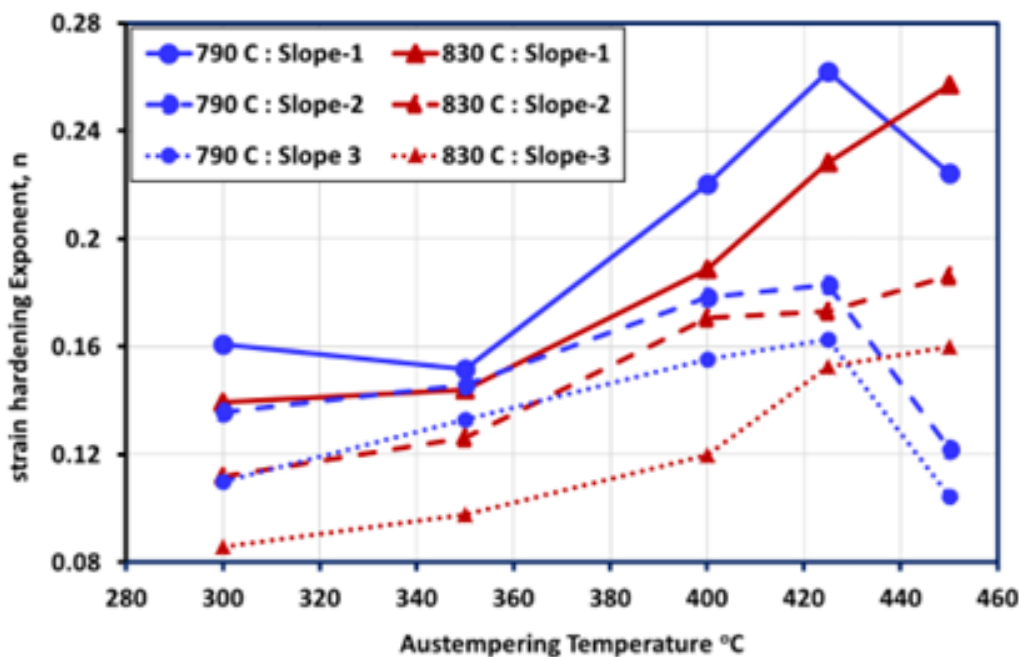


Figure 11(b): The effect of austempering temperature on the strain hardening exponent as per Hollomon equation.

The modified Crussard Jaoul analysis model for work hardening is based on earlier studies [10]

$$\epsilon = \epsilon_0 + c\sigma^m \quad (3)$$

Where ϵ is true strain; ϵ_0 is the initial strain and σ is the true stress and the exponent m is inverse of the strain hardening exponent. In the differential form, the above equation translates to

$$\ln(d\sigma / d\epsilon) = (1 - m) \ln \sigma - \ln(cm) \quad (4)$$

The plot between the work hardening rate and true stress is given by the plots in Figure 12(a) & (b). The graph shows three distinct region of work hardening. The slopes determined the value of $(1-m)$ from which n values were determined. The n values found from CJ model as a function of austempering temperature is shown in Figure 12(b). The results show variation from Hollomon model. It is seen that after achieving a maximum work hardening, there is a fall in work hardening rate as per CJ model, which was not evident in Hollomon model.

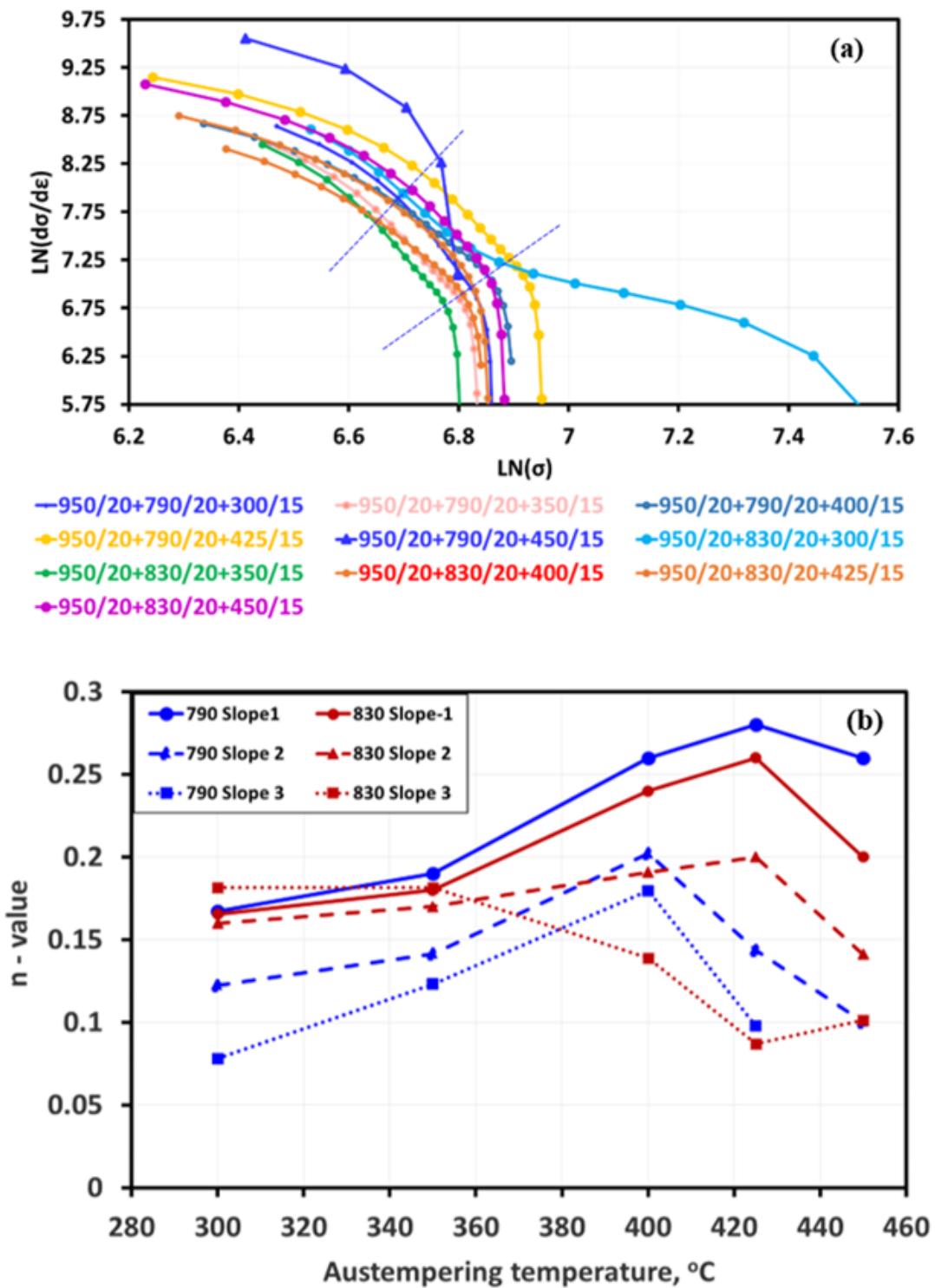


Figure 12: The work hardening of the steel at the various processing conditions (a) as per the modified Crussard Jaoul Model. (b) The effect of austempering temperature on the work hardening coefficient derived from CJ Model.

It is seen that the strength and ductility combination is greater than or equal to 20GPa.% when the steel was pre-quenched, intercritically austenitized followed by austempering (Figure 10). Unlike our previous study where 3rd Gen AHSS could be realized only at 425 °C [11], the present study gives consistent properties in most conditions the 3rd Gen AHSS range.

Conclusion

1. The mechanical properties of a lean alloyed TRIP steel pre hardened and intercritically austenitized at 830 and 790 °C, was austempered between 300 and 450 °C. The microstructure of the steel was estimated from the SEM microstructure. The

ferrite content varied between 28 and 62%, the bainitic ferrite between 14 and 45%, the M/A constituents varied between 4 and 17% and the retained austenite content varied between 4 and 18%.

2. The bainite evolution during austempering was assessed theoretically by evaluation of the T_0' temperature and the bainite fraction. The actual bainite content measured and evaluated was significantly differing probably because of a secondary transformation of the retained austenite post austempering.
3. The mechanical properties of the steel in the austempered condition shows 766 to 968 MPa with 20 to 29% elongation with yield ratio between 0.57 to 0.72.
4. The work hardening behaviour was assessed using the Hollomon equation and modified Crussard Jaoul model. Both the models show three distinct regions of work hardening associated with the different phase constituents.

References

1. Arif B, Etienne A (1999) Influence of rolling of TRIP steel in the inter critical region on the stability of retained austenite. *Journal of Materials Processing Technology* 89-90: 37-43.
2. Nemecek S, Novy Z, Stankova H (2005) 2nd International conference heat treatment and surface engineering in automotive applications. *La Metallurgia Italiana*, Riva del Garda, Italy, pp. 47-52
3. Li Z, Wu D (2008) Effects of hot deformation and subsequent austempering on mechanical properties of high silicon and low silicon TRIP steel. *Materials Science and Technology* 24(2): 168-176.
4. Jozef Z, Ondrej M, Ondrej S, Peter L, Peter H (2008) Effect of processing conditions on structure development and mechanical response of Si-Mn 'TRIP' steel. *Materials Science and Engineering A* 483-484: 71-75.
5. Lin L, Ed by Yuqing W, Han D, Yong G (2011) *Advanced steels - the recent scenario in steel science and technology*. Springer Springer-Verlag Berlin Heidelberg and Metallurgical Industry Press.
6. Kucerova L, Bystriansky M (2016) *The Journal of Achievements in Materials and Manufacturing Engineering* 77: 5-12.
7. Rui D, Aimin Z, Ran D, Jianguo H, Hanjiang H (2015) Microstructure and mechanical properties of TRIP-aided steels with different heat treatments. *Materials Science Forum* 817: 439-443.
8. Law NC, Edmonds DV (1980) The formation of austenite in a low-alloy steel. *Metallurgical and Materials Transactions A* 11: 33-46.
9. <https://www.phasetrans.msm.cam.ac.uk/map/steel/programs/mucg83.html>
10. Xiong ZP, Kostryzhev AG, Saleh AA, Chen L, Pereloma EV (2016) Microstructures and mechanical properties of TRIP steel produced by strip casting simulated in the laboratory. *Materials Science and Engineering A: Structural Materials: Properties, Microstructure and Processing* 664: 26-42.
11. Mohapatra JN, Satish KD, Balachandran G (2022) Development of a lean alloyed TRIP assisted bainitic steel by austempering treatment. *Trans Indian Inst Met* 75: 229-238.